Electronic Supplementary Material (ESI) for Soft Matter.
This journal is © The Royal Society of Chemistry 2023

Supplementary Information

^{1}H-NMR studies on the volume phase transition of DNA-modified pNipmam microgels

Rebecca Hengsbach, Gerhard Fink, Ulrich Simon

Institute of Inorganic Chemistry, RWTH Aachen University, Landoltweg 1a, D-52074 Aachen, Germany.

Experimental

The DNA-functionalization of µG is shown schematically in Figure S1.

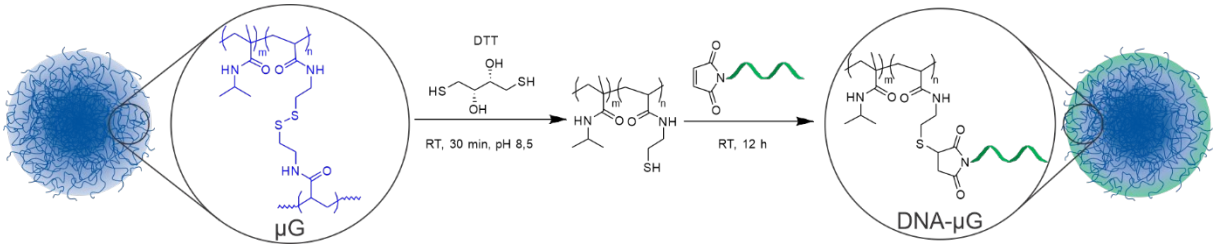

Figure S1: Reaction scheme of the DNA-functionalization of the µG.

SEM-Measurements

The µG and DNA-µG were examined in a FE-SEM LEO/Zeiss Supra 35 VP. For this a 10 µL droplet of the dispersions (0.2mg/mL) was dried on cleaned Silicon wafers (Figure S2). Cleaning was done by boiling in a water:ammonia:hydrogen peroxide mixture (3:1:1), washing with water and drying with nitrogen.

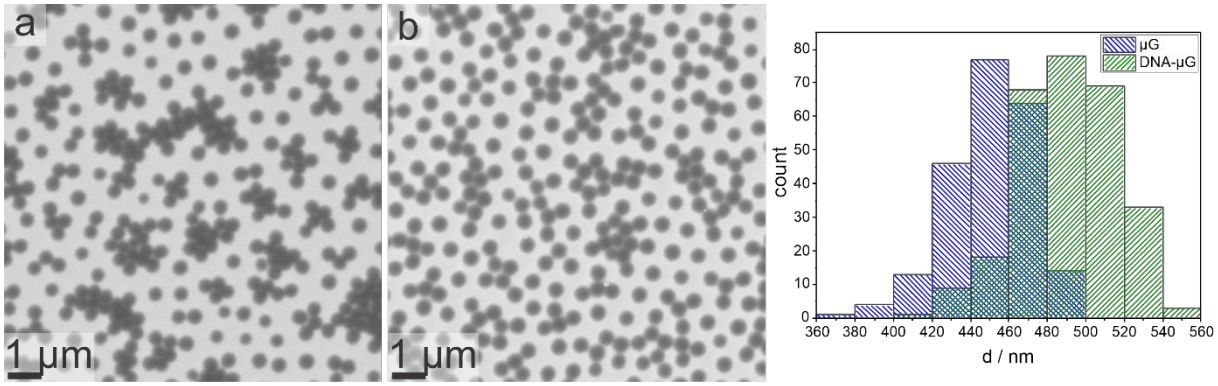

Figure S2: SEM images (InLens-detector) of the µG (a) and the DNA-µG (b) with corresponding histogram.

The DNA-µG show a slightly bigger diameter in the dried state than the pure ones (Table S1). This can be explained by the negative charges of the DNA which leads to a repulsion inside of the DNA-µG. The diameter was determined for at least 200 µG for each sample.

Table S1: Diameter of the µG (a), the DNA-µG (b) in the dried state.

sample	diameter / nm
a	450 ± 20
b	490 ± 20

DLS-Measurements

The µG and DNA-µG were investigated via DLS (Malvern Zetasizer NanoS, HeNe-laser λ = 633 nm, P = 4 mW) by measuring the hydrodynamic diameter in dependency of the temperature in adjusted salt concentrations in UV-microcuvettes (Brand) with Θ = 173°. Using this kind of measurement, the VPTT of the sample can be determined by the turning point of the curves by using a sigmoidal fit function in Origin 2021b (Figure S3).

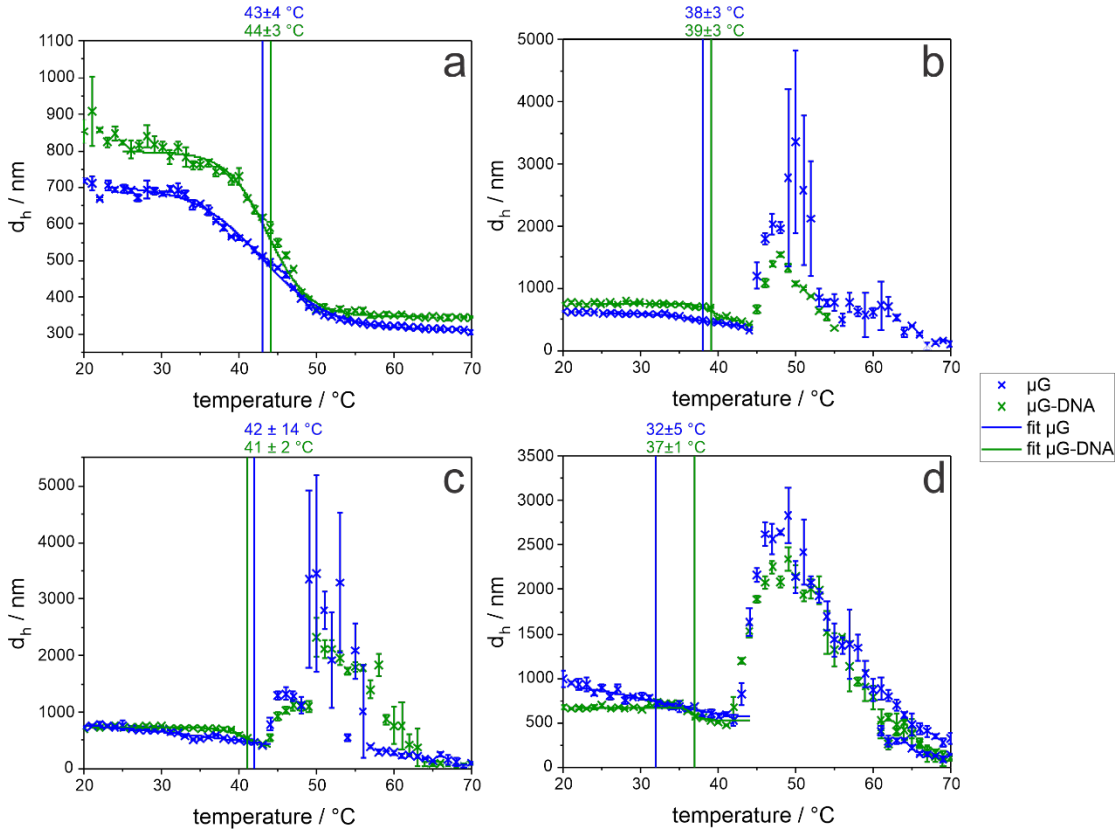

Figure S3: Hydrodynamic diameters in dependency of the temperature of the µG and the DNA-µG with fitted regions for the determination of the VPTT in H_2O (a) in 0.1 M NaCl (b) in 0.14 M NaCl (c) and in PBS (d) with the VPTT indicated by vertical lines.

At lower temperatures the hydrodynamic diameter of the µG in the swollen state can be observed and at higher temperatures the collapse of the µG accompanied by smaller sizes can be seen. The DNA-µG show higher diameters in water which can be explained by the repelling forces of DNA inside µG. [1] During DNA functionalization the amount of crosslinker inside the µG is lowered which does not shift the VPTT

significantly (Table S2) but could lead to a more pronounced swelling with decreasing crosslinker amount. [2] During the collapse of the µG there is a distribution of different sizes of µG in the sample. [3] With added salt an aggregation of all samples above the VPTT occurs which is indicated by rising diameters. The aggregates settle down which leads to a decrease in diameter again. Caused by the aggregation the determination of the VPTT gets more difficult with higher salt concentration. NMR measurements are not influenced by the aggregation behavior and therefore better suited for examinations in salt solutions. For a better comparison all DLS-measurements are summarized in Figure S4.

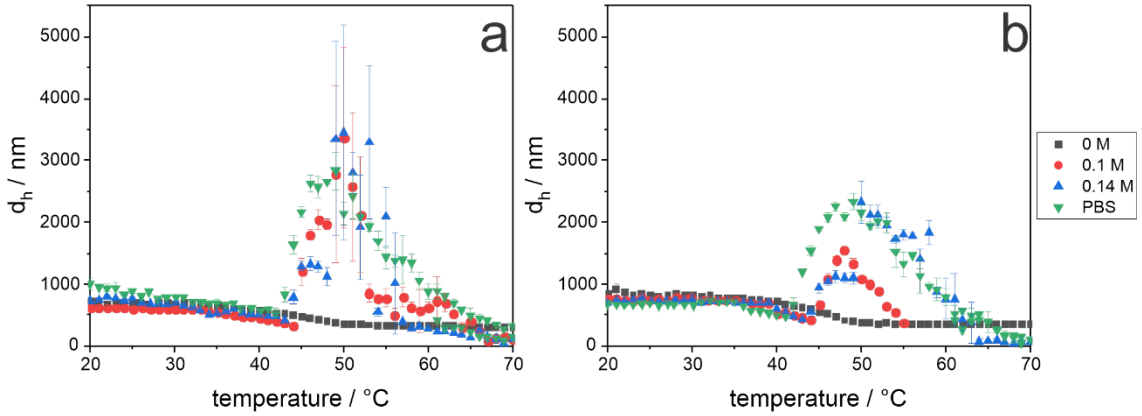

Figure S4: Hydrodynamic diameter in dependency of the temperature for the µG (a) and the DNA-µG (b) at adjusted salt concentrations.

The VPTT of the different samples are summarized in Table S2.

Table S2: VPTT of the µG and DNA-µG determined by DLS at adjusted salt concentrations.

salt concentration	VPTT / °C	
	pNipmam	pNipmam-DNA
0 M	41 ± 5	44 ± 3
0.1 M	38 ± 3	41 ± 2
0.14 M	42 ± 14	41 ± 2
PBS	32 ± 5	37 ± 1

The VPTT is decreasing with increasing salt concentration. All of these values need to be handled carefully caused by the uncertainties in determination reasoned by the aggregation which can be seen in high fitting errors.

Fluorescence Microscopy

To verify the DNA functionalization of the DNA-µG Atto647 labeled complementary ssDNA (5'-CGC ATT CAG GAT AAA AAA AAA A-3'-Atto647, 10 µL, 100 µM, biomers) was added to the DNA-µG (50 µL). The hybridization was done by incubation of the DNA-µG with complementary ssDNA for 12 h at 4 °C. The sample was washed 3 times with sodium chloride solution (1 M) and three times with water with centrifugation at 10.000 rpm, 10 min, 20 °C in a Thermoscientific Heraeus Fresco 21 microcentrifuge with 1.5 mL Eppendorf tubes. The sample was redispersed in water. Fluorescence microscopy was performed on a Nikon Eclipse Ti-E with a 100×/1.40 NA oil immersion objective (HP PLAN, Nikon) and imaged on a CMOS camera (Photometrics, PRIME 95B). To observe the localization of the dyes inside the

DNA-µG they were observed in transmission mode and the dyes in a fluorescence image with a 640 nm laser (Toptica iBeam smart 640CD) with a laser power of 200 mW. (Figure S5).

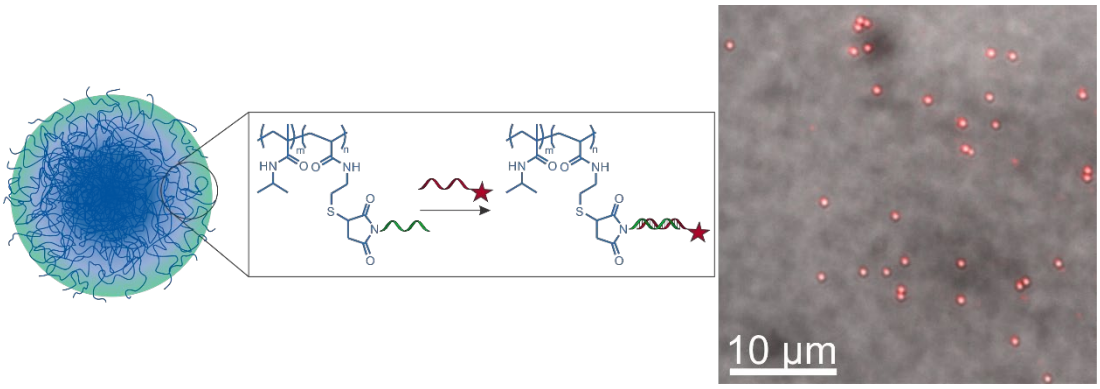

Figure S5: Schematic illustration of the hybridization of fluorescent labelled ssDNA inside of DNA-µG (left) and overlay of brightfield microscopy (grey) and fluorescence microscopy (red) image of the DNA-µG after hybridization with labeled DNA (right).

The red color indicates the fluorescent dye which is located in the DNA-µG. Without a hybridization the labeled ssDNA would have been washed away. [1]

NMR-measurements

As the magnetic field is permanently corrected by the spectrometer to keep the deuterium signal of the solvent (D_2O) at the same spectral position ("locked") and the absolute resonance frequency of water is changing with temperature, all peaks, except for water, are moving in the spectrum. The observed linear drift was corrected manually using the spectral referencing parameter in Topspin ('sr'). A twofold automatic phase correction was done.

The signal intensities of the NMR measurements at different temperatures are summarized in Figure S6.

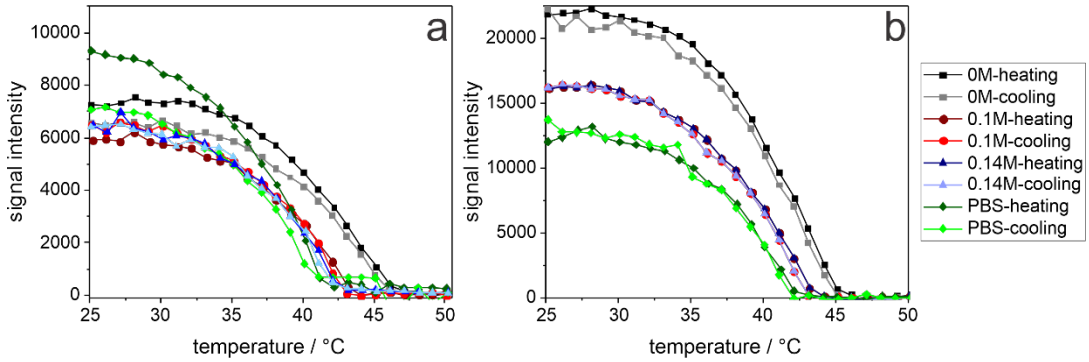

Figure S6: Signal intensities of the NMR-spectra of the µG (a) and the DNA-µG (b).

Since the intensities of the NMR spectra for the 0.1 M and 0.14 M sodium chloride solutions of the DNA-µG are similar they are overlapping.

The van't Hoff plot is shown in Figure S7 for the µG and DNA-µG at adjusted salt concentrations.

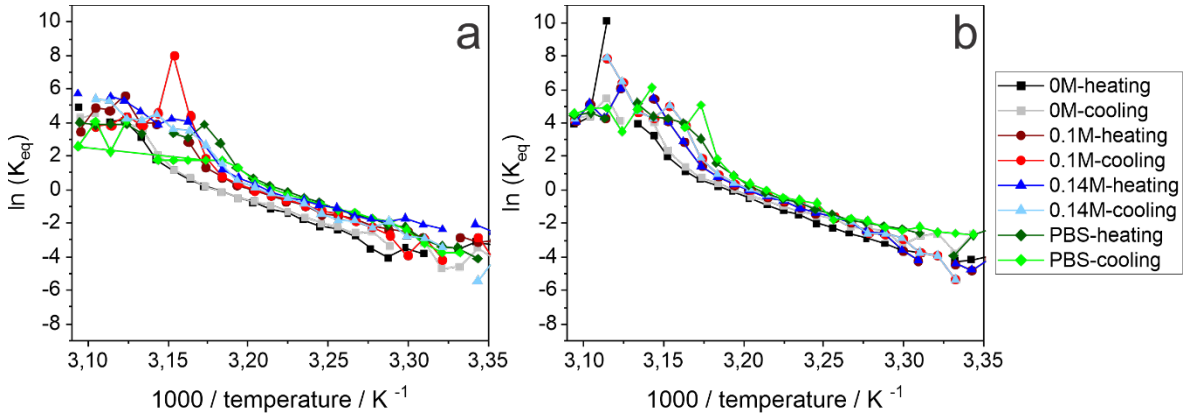

Figure S7: Van't Hoff Plots of the NMR-spectra of the µG (a) and the DNA-µG (b) at adjusted salt concentrations.

In the van't Hoff plot a linear fit can be applied for the determination of the thermodynamic values (Figure S8). The values from Table S5 are used to set the borders for the fits.

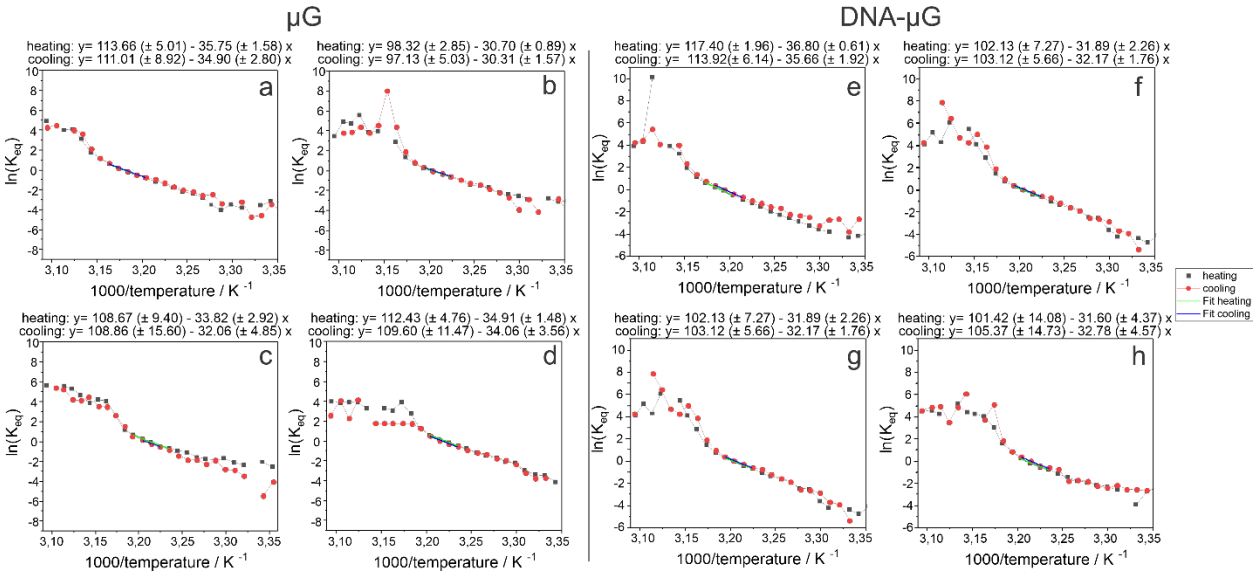

Figure S8: Van't Hoff Plots [1]with fitted linear regions of the µG in D_2O (a) in 0.1 M NaCl (b) in 0.14 M NaCl (c) and in PBS (d) and of the DNA-µG in D_2O (e) in 0.1 M NaCl (f) in 0.14 M NaCl (g) and in PBS (h).

The slope and interception for the linear equations are summarized in Table S3.

Table S3: Interceptions and slopes of the fitted linear equation in van't Hoff plots for the µG and the DNA-µG at adjusted salt concentrations.

			interception	error	slope	error
µG	0M	heating	113.66	5.01	-35.75	1.58
		cooling	111.01	8.92	-34.90	2.80
	0.1M	heating	98.32	2.85	-30.70	0.89
		cooling	97.13	5.03	-30.31	1.57
	0.14M	heating	108.67	9.39	-33.82	2.92
		cooling	102.86	15.59	-32.06	4.85
	PBS	heating	112.43	4.76	-34.91	1.48
		cooling	109.60	11.47	-34.06	3.56

µG-DNA	0M	heating	117.40	1.96	-36.80	0.61
		cooling	113.92	6.14	-35.66	1.92
	0.1M	heating	102.13	7.27	-31.89	2.26
		cooling	103.12	5.66	-32.17	1.76
	0.14M	heating	102.13	7.27	-31.89	2.26
		cooling	103.12	5.66	-32.17	1.76
	PBS	heating	101.42	14.08	-31.60	4.37
		cooling	105.37	14.73	-32.78	4.57

Using the slope and interception of the linear equations the thermodynamic values can be determined using equations (S1), (S2).

$$\Delta \mathrm{H} = -R \cdot slope \qquad (S1)$$

$$\Delta \mathrm{S} = R \cdot intercept \qquad (S2)$$

Additionally, the changes in Gibbs free energy were determined and the resulting thermodynamic values are summarized in Table S4 (Figure S9).

Table S4: Thermodynamic values for the µG and the DNA-µG at adjusted salt concentrations determined via linear fit.

			ΔH kJ/mol	error	ΔS J/ mol·K	error	ΔG (298K) kJ/mol	error
µG	0 M	heating	297.23	13.14	944.97	41.65	15.62	0.72
		cooling	290.16	23.28	922.94	74.16	15.12	1.18
	0.1 M	heating	255.24	7.40	817.43	23.69	11.64	0.34
		cooling	252.00	13.05	807.54	41.82	11.35	0.59
	0.14 M	heating	281.20	24.30	903.52	78.11	11.96	1.02
		cooling	266.55	40.34	855.20	129.65	11.70	1.70
	PBS	heating	290.24	12.30	934.74	39.57	11.69	0.51
		cooling	283.17	29.60	911.21	95.36	11.63	1.18
µG-DNA	0 M	heating	305.96	5.07	976.06	16.30	15.09	0.22
		cooling	296.48	15.96	947.13	51.05	14.23	0.75
	0.1 M	heating	265.13	18.79	849.11	60.44	12.10	0.78
		cooling	267.46	14.63	857.34	47.06	11.97	0.61
	0.14 M	heating	265.13	18.79	849.11	60.44	12.10	0.78
		cooling	267.46	14.63	857.34	47.06	11.97	0.61
	PBS	heating	262.72	36.33	843.21	117.06	11.45	1.45
		cooling	272.53	37.99	876.05	122.47	11.47	1.50

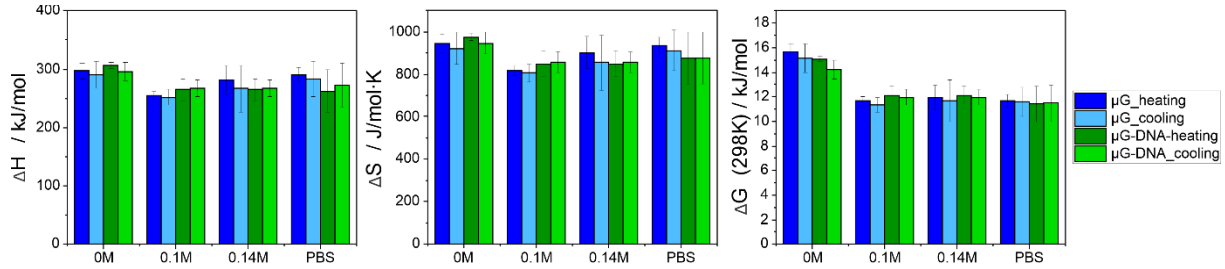

Figure S9: Thermodynamic values determined via linear fits at adjusted salt concentrations for the µG and the DNA-µG.

The change in Gibbs free energy is decreasing with increasing salt concentration. The sample without added salt shows lower energies for the DNA-µG than for the µG and there is a hysteresis between heating and cooling which is in accordance with literature. [4-6] ΔG is positive for all samples which is in accordance with the VPTT since there is no spontaneous collapse at 25 °C.

To be able to do the non-linear fit it is necessary to determine the most accurate measurement data points Int_1 and Int_2 which is done with equation (S3).

$$(1 - Int_1) \cdot (Int_1 - 0) \cdot (1 - Int_2) \cdot (Int_2 - 0) \cdot |Int_1 - Int_2| \qquad (S3)$$

The 3D visualization of the most accurate values to use for the non-linear fit are shown in Figure S10. These values were additionally used as borders for the linear fit via van't Hoff plot. Two data points are determined which are far from 0 and 1 and far from each other.

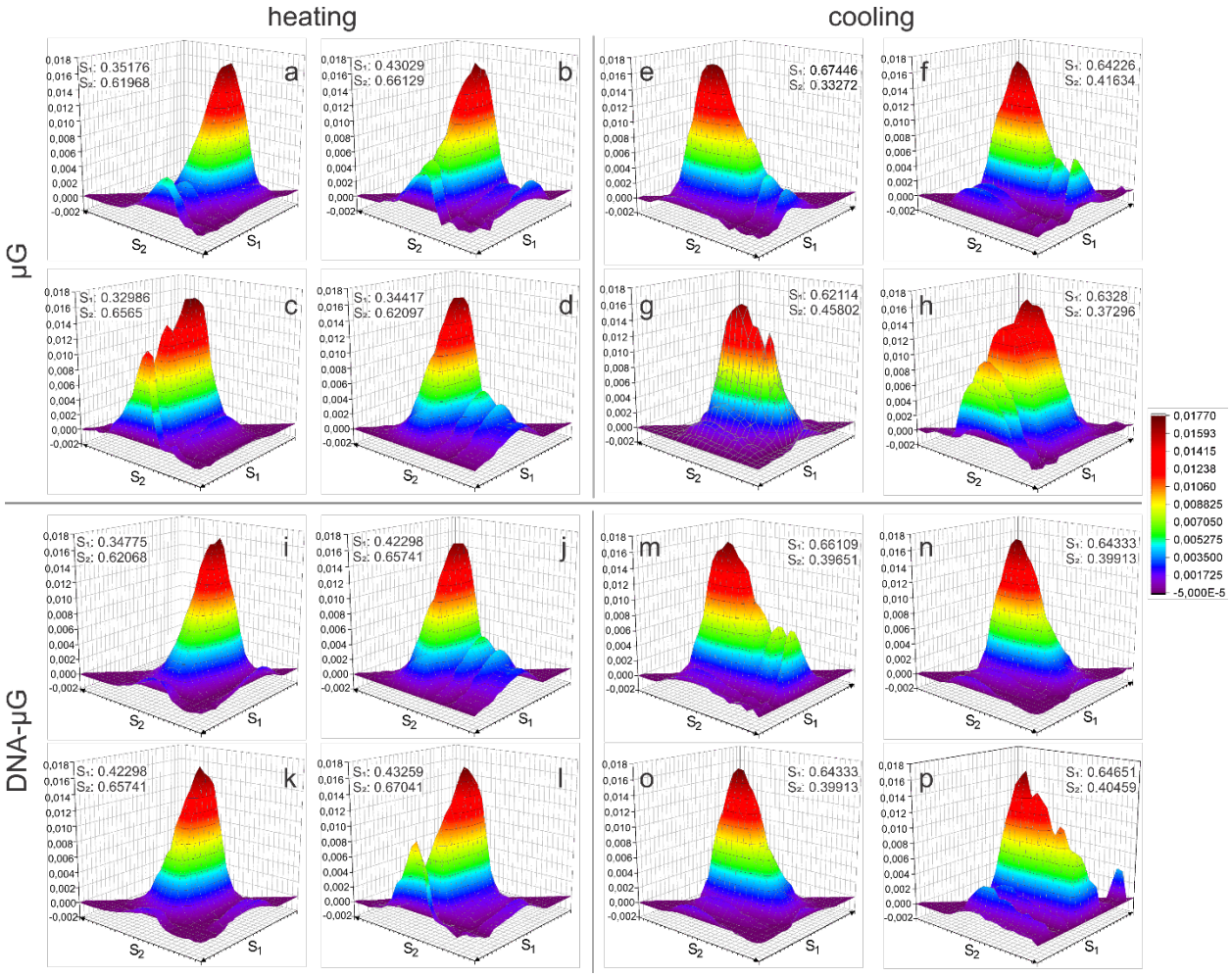

Figure S10: Visualization of best suited values for the determination of the thermodynamic values of the μG in D_2O (a) in 0.1 M NaCl (b) in 0.14 M NaCl (c) and in PBS (d) for the heating experiment and in D_2O (e) in 0.1 M NaCl (f) in 0.14 M NaCl (g) and in PBS (h) for the cooling experiment and of the DNA-μG in D_2O (i) in 0.1 M NaCl (j) in 0.14 M NaCl (k) and in PBS (l) for the heating experiment and in D_2O (m) in 0.1 M NaCl (n) in 0.14 M NaCl (o) and in PBS (p) for the cooling experiment.

The resulting values are summarized in Table S5 and the corresponding equilibrium constants $K_{eq}(T)$ are calculated with equation (S4).

$$K_{eq}(T) = \frac{Int\ (298K) - Int(T)}{Int(T)} \qquad (S4)$$

Table S5: Summary of the most accurate values for determination of the thermodynamic values for the μG and DNA-μG.

			T / K	Int	$K_{eq}(T)$	T / K	Int	$K_{eq}(T)$
μG	0M	heating	316.1	0.35176	1.84	313.3	0.61968	0.61
		cooling	316.1	0.33272	2.01	312.1	0.67446	0.48
	0.1M	heating	313.2	0.43029	1.32	310.2	0.66129	0.51
		cooling	313.1	0.41634	1.40	310.2	0.64226	0.56
	0.14M	heating	309.1	0.6565	0.52	313.1	0.32986	2.03
		cooling	310.1	0.62114	0.61	312.1	0.45802	1.18
	PBS	heating	312.2	0.34417	1.91	309.1	0.62097	0.61

		cooling	312.1	0.37296	1.68	309.1	0.6328	0.58
µG-DNA	0M	heating	315.2	0.34775	1.88	312.2	0.62068	0.61
		cooling	314.1	0.39651	1.52	311.1	0.66109	0.51
	0.1M	heating	313.1	0.42298	1.36	310.1	0.65741	0.52
		cooling	313.1	0.39913	1.51	310.1	0.64333	0.55
	0.14M	heating	313.1	0.42298	1.36	310.1	0.65741	0.52
		cooling	313.1	0.39913	1.51	310.1	0.64333	0.55
	PBS	heating	312.2	0.43259	1.31	309.2	0.67041	0.49
		cooling	312.1	0.40459	1.47	309.1	0.64651	0.55

The equilibrium constants can be used to calculate pairs of enthalpy ΔH and entropy ΔS according to equation (S5) with the temperature T and the gas constant R.

$$\Delta \mathrm{H} = \Delta S \cdot T - T \cdot R \cdot lnK_{eq} \qquad (S5)$$

Using equation (S5) for both determined equilibrium constants with the corresponding temperatures two linear graphs for each measurement can be drawn and the intersection can be determined for a first estimation of ΔH and ΔS (Figure S11).

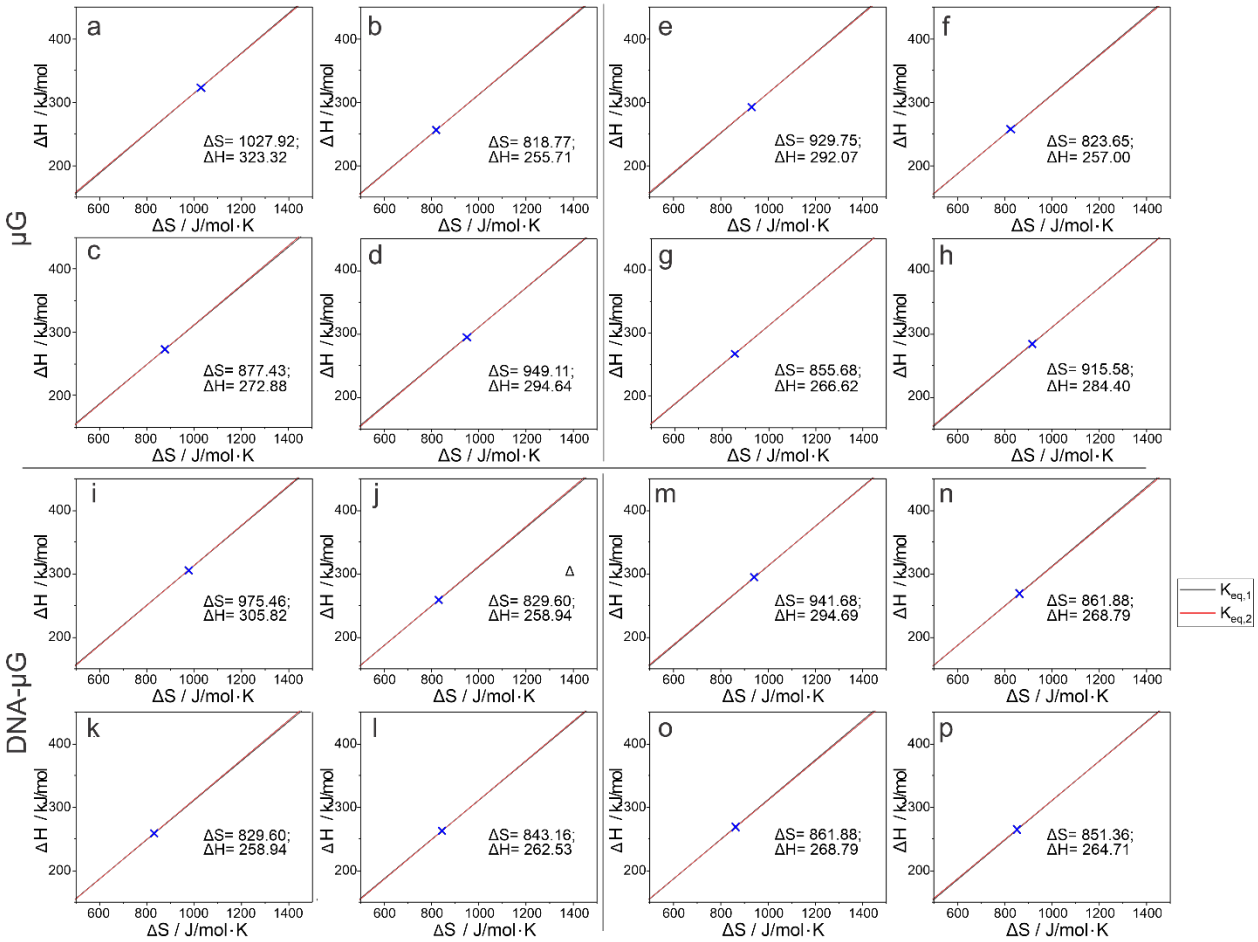

Figure S11: First estimation of changes of entropy- and enthalpy values for the fit of the thermodynamic values of the µG in D_2O (a) in 0.1 M NaCl (b) in 0.14 M NaCl (c) and in PBS (d) for the heating experiment and in D_2O (e) in 0.1 M NaCl (f) in 0.14 M NaCl

(g) and in PBS (h) for the cooling experiment and of the DNA-µG in D_2O (i) in 0.1 M NaCl (j) in 0.14 M NaCl (k) and in PBS (l) for the heating experiment and in D_2O (m) in 0.1 M NaCl (n) in 0.14 M NaCl (o) and in PBS (p) for the cooling experiment.

These values for ΔH and ΔS will be used as starting point for the non-linear fit with four unknown variables.

The non-linear fit is done using equation (S8) which was obtained by combining equation (S6) where the equilibrium constant and the relative signal intensity are related and equation (S7) which correlates the equilibrium constant to ΔH and ΔS.

$$Int = Int_0 + Int_1 \cdot \frac{1}{K_{eq} + 1} \quad (S6)$$

$$K_{eq} = e^{-\frac{\Delta H}{RT} + \frac{\Delta S}{R}} \quad (S7)$$

$$Int = Int_0 + Int_1 \cdot \frac{1}{1 + e^{-\frac{\Delta H}{T \cdot R}} \cdot e^{\frac{\Delta S}{R}}} \quad (S8)$$

The non-linear fit was done in Origin 2021b by setting two of the four unknown variables at starting points. These were estimated for ΔH and ΔS before. First Int_0 and Int_1 were fitted. In a second step these values can be used to refit ΔH and ΔS and afterwards all four variables are fitted together (Figure S12). Int_0 and Int_1 were used to exclude measurement errors which might occur around 0 and 1.

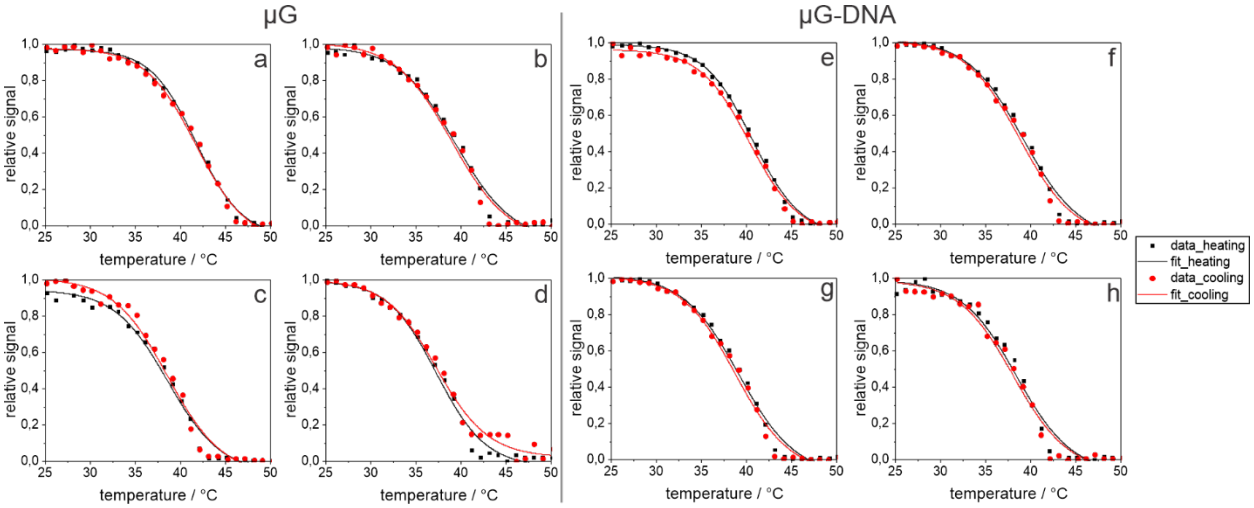

Figure S12: Non-linear fit of the thermodynamic values of the µG in D_2O (a) in 0.1 M NaCl (b) in 0.14 M NaCl (c) and in PBS (d) and of the DNA-µG in D_2O (e) in 0.1 M NaCl (f) in 0.14 M NaCl (g) and in PBS (h).

The values determined by the non-linear Fit are summarized in Table S6 and visualized in Figure S13.

Table S6: Fitted Int_0, Int_1, ΔH and ΔS for the µG and the DNA-µG at adjusted salt concentrations.

			Int_0	error	Int_1	error	ΔH / kJ/mol	error	ΔS / J/mol*K	error
µG	0M	heating	-0.07	0.02	1.04	0.02	323.65	0.58	1028.20	1.60
		cooling	-0.10	0.03	1.08	0.03	291.39	0.88	925.77	2.41
	0.1M	heating	-0.09	0.03	1.08	0.05	255.16	1.34	816.62	4.03
		cooling	-0.09	0.04	1.10	0.05	255.47	1.44	818.71	4.39
	0.14M	heating	-0.07	0.03	1.02	0.04	271.12	1.23	870.02	3.79
		cooling	-0.08	0.03	1.10	0.04	265.90	1.30	853.20	4.02

	PBS	heating	-0.03	0.02	1.03	0.03	293.44	0.94	945.61	3.02
		cooling	0.02	0.02	0.98	0.03	281.29	1.04	906.43	3.35
µG-DNA	0M	heating	-0.07	0.02	1.06	0.02	305.52	0.64	973.92	1.85
		cooling	-0.07	0.02	1.04	0.03	293.58	0.84	936.80	2.46
	0.1M	heating	-0.09	0.03	1.11	0.04	258.46	1.13	827.75	3.41
		cooling	-0.08	0.03	1.09	0.04	267.41	1.12	857.50	3.43
	0.14M	heating	-0.09	0.03	1.11	0.04	258.46	1.13	827.75	3.41
		cooling	-0.08	0.03	1.09	0.04	267.41	1.12	857.50	3.43
	PBS	heating	-0.08	0.03	1.07	0.05	262.41	1.45	842.41	4.49
		cooling	-0.07	0.03	1.06	0.05	264.59	1.50	850.42	4.71

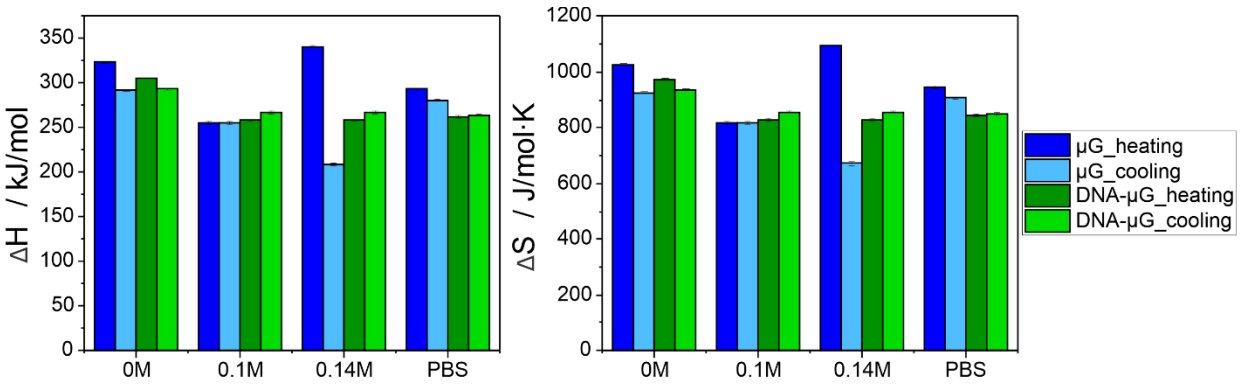

Figure S13: Thermodynamic values determined via non-linear fit at adjusted salt concentrations for the µG and the DNA-µG.

The changes in Gibbs free energy determined by the two different fitting methods are compared in Table S7 and Figure S14.

Table S7: Changes in Gibbs free energy determined by non-linear and linear fits for the µG and the DNA-µG at adjusted salt concentrations.

			non-linear fit		linear fit	
			ΔG (298 K) kJ/mol	error	ΔG (298K) kJ/mol	error
µG	0 M	heating	17.25	0.10	15.62	0.72
		cooling	15.51	0.16	15.12	1.18
	0.1 M	heating	11.81	0.14	11.64	0.34
		cooling	11.49	0.13	11.35	0.59
	0.14 M	heating	15.09	0.05	14.95	0.81
		cooling	9.01	0.17	9.58	0.79
	PBS	heating	11.64	0.04	11.69	0.51
		cooling	11.17	0.04	11.63	1.18
µG-DNA	0 M	heating	15.29	0.09	15.09	0.22
		cooling	14.41	0.11	14.23	0.75
	0.1 M	heating	11.79	0.11	12.10	0.78
		cooling	11.87	0.10	11.97	0.61
	0.14 M	heating	11.79	0.11	12.10	0.78
		cooling	11.87	0.10	11.97	0.61

	PBS	heating	11.37	0.11	11.45	1.45
		cooling	11.16	0.10	11.47	1.50

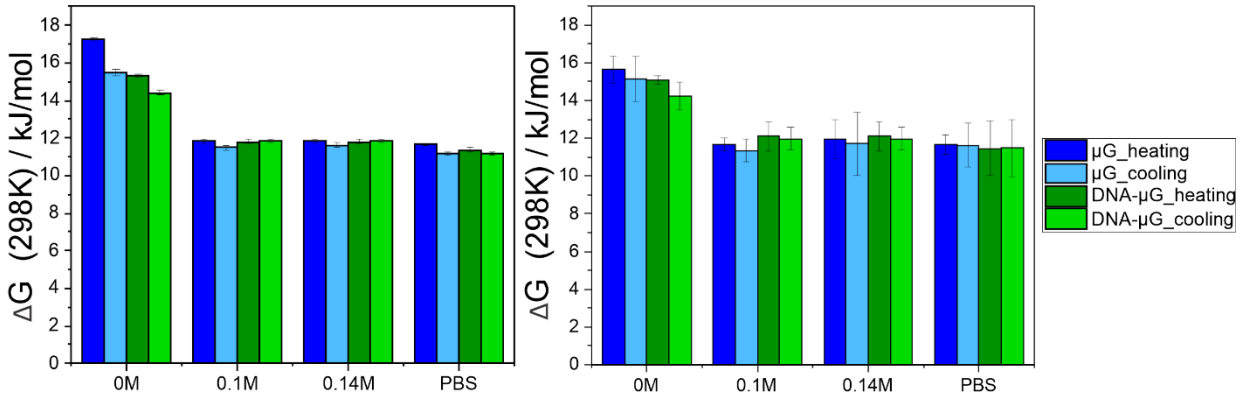

Figure S14: Changes in Gibbs free energy determined by non-linear (left) and linear (right) fits for the μG and the DNA-μG at adjusted salt concentrations.

References

1. Eisold, S.; Hoppe Alvarez, L.; Ran, K.; Hengsbach, R.; Fink, G.; Centeno Benigno, S.; Mayer, J.; Woll, D.; Simon, U., DNA introduces an independent temperature responsiveness to thermosensitive microgels and enables switchable plasmon coupling as well as controlled uptake and release. *Nanoscale* **2021,** *13* (5), 2875-2882.
2. Zeiser, M.; Freudensprung, I.; Hellweg, T., Linearly thermoresponsive core–shell microgels: Towards a new class of nanoactuators. *Polymer* **2012,** *53* (26), 6096-6101.
3. Zhang, Y.; Furyk, S.; Bergbreiter, D. E.; Cremer, P. S., Specific Ion Effects on the Water Solubility of Macromolecules: PNIPAM and the Hofmeister Series. *J. Am. Chem. Soc.* **2005,** *127*, 14505-14510
4. Burba, C. M.; Carter, S. M.; Meyer, K. J.; Rice, C. V., Salt Effects on Poly(N-isopropylacrylamide) Phase Transition Thermodynamics from NMR Spectroscopy. *J. Phys. Chem. B* **2008,** *112* 10399–10404.
5. Pastoor, K. J.; Rice, C. V., Anion effects on the phase transition of N-isopropylacrylamide hydrogels. *Journal of Polymer Science Part A: Polymer Chemistry* **2012,** *50* (7), 1374-1382.
6. Pastoor, K. J.; Rice, C. V., Cation Effects on the Phase Transition of N-isopropylacrylamide Hydrogels. *Macromol Chem Phys* **2015,** *216* (9), 1024-1032.